Journal of Inflammation Research

Dovepress
Taylor & Francis Group

Open Access Full Text Article

ORIGINAL RESEARCH

IRF6 Enhances IFN-β Expression and Inhibits Viral Replication to Reduce the Severity of Herpetic Stromal Keratitis

Zhi Liu, Likun Xia

Department of Ophthalmology, Shengjing Hospital of China Medical University, Shenyang, Liaoning, People's Republic of China

Correspondence: Likun Xia, Email xialk@sj-hospital.org

Purpose: Herpes simplex virus type 1 (HSV-1) infection of the human eye can lead to herpes simplex keratitis, which is the leading cause of infectious blindness worldwide. Inflammation invading the corneal stroma causes herpetic stromal keratitis (HSK). Interferon regulatory factor 6 (IRF6) is a member of the interferon regulatory factor family and is involved in the antiviral response against human papillomavirus 16. However, the mechanism related to the involvement of IRF6 in the host anti-HSV-1 response is unclear, and how latent infection and viral reactivation trigger corneal stromal inflammation remains unknown. Therefore, we investigated the role of IRF6 in HSV-1 infection.

Methods: Proteomic detection techniques indicated that IRF6 was expressed at low levels in the corneas of HSK model mice. The antiviral effects of IRF6 have been demonstrated in animal and cellular studies. HSV-1 replication was activated when IRF6 was silenced in human corneal epithelial cells (HCECs), and IRF6 overexpression inhibited viral replication. HSK was established after locally inoculating mouse corneas with lentivirus to overexpress IRF6.

Results: The degree of inflammation was attenuated, and proinflammatory cytokine secretion was reduced in the mice overexpressing IRF6 compared with that in the lentivirus control mice, suggesting that IRF6 attenuates the severity of HSK. Silencing of protein kinase C delta and receptor-interacting serine/threonine kinase 4 reduced IRF6 phosphorylation and inhibited its degradation during HCEC infection with HSV-1.

Conclusion: These findings indicate that IRF6 is involved in the immune response against HSV-1 virus, and IRF6 can be used as a therapeutic target for treating HSK.

Keywords: HSV-1, herpetic stromal keratitis, Keratitis, IRF6, innate immunity

Introduction

Herpes simplex virus (HSV) is a double-stranded DNA virus that infects nervous tissue.[1,2] HSV can be divided into two subtypes: HSV-1 and HSV-2. HSV-1 mainly infects the oral mucosa and eyes, while HSV-2 mainly infects reproductive organs. Humans are the only natural hosts of HSV-1, and the rate of HSV-1 seropositivity in the population is as high as 50–90%.[3] HSV-1 infection of the human eye can lead to herpes simplex keratitis, which is difficult to control effectively, prone to recurrent episodes, and is the main cause of blindness in human infectious keratopathies.[4,5] Globally, approximately 1.5 million ocular HSV cases are reported annually, resulting in 40,000 people becoming blind.[4] HSV-1 infections are categorized into two types: primary and recurrent. HSV-1 directly contacts the mucous membrane and causes primary infection, which is mild and easy to control. The virus then reaches the trigeminal ganglion by reverse axonal transport and establishes lifelong latency.[6] Reactivation of the virus causes a large number of inflammatory cells to infiltrate the cornea, resulting in herpetic stromal keratitis (HSK). Herpetic stromal keratitis is characterized by corneal clouding, edema, corneal scarring, and neovascularization, all of which directly affect vision. Antiviral and anti-inflammatory combination therapies are used to treat HSK; however, specific therapeutic drugs are lacking, and immunocompromised individuals may be more susceptible to developing drug resistance.[7,8] No effective vaccine

Received: 4 April 2025
Accepted: 25 August 2025
Published: 2 September 2025

currently exists to prevent HSV-1 infections,[9,10] and no effective treatment that can completely eliminate the virus from the latent sites.[11] Therefore, effectively suppressing viral replication and reducing the excessive inflammatory response triggered by viral invasion are keys to disease control.

Interferon regulatory factors (IRFs) are transcription factors that regulate the expression of type I interferons (IFNs) and related genes and play essential roles in immune regulation and inflammatory responses. In addition, IRFs are involved in regulating cell growth, differentiation, apoptosis, tumorigenesis, and metabolism.[12–16] Nine IRF species have been identified in mammals.[17] IRF proteins contain two functional domains: an N-terminal helix-turn-helix DNA-binding domain containing conserved tryptophan residues and a C-terminal interferon activation domain (IAD, also known as the IRF-association domain), which mediates IRFs. Tryptophan residues and a C-terminal IAD mediate protein-protein interactions.[18,19] IRF6 is a member of the IFN regulatory factor family. IRF6 is a key regulator of epithelial cell proliferation and differentiation,[20] and is crucial for epithelial barrier function in mammals;[21] however, no evidence exists that IRF6 acts by regulating IFN gene expression. Mutations in the IRF6 gene cause Van der Woude syndrome and popliteal pterygium syndrome (PPS). The ocular manifestation of PPS is pterygium.[22] Receptor-interacting protein kinase 4 (RIPK4) is a receptor-interacting protein kinase family member. RIPK4 has serine/threonine protein kinase activity and interacts with protein kinase C-β and protein kinase C delta (PKD).[23] RIPK4, which PKC activates, regulates keratinocyte differentiation and inflammation-related responses by modulating IRF6 phosphorylation.[24,25] IRF6 and RIPK4 are key factors involved in regulating keratinocyte differentiation.[24] IRF6 plays a role in the antiviral response by regulating interleukin (IL)-1β promoter activity in human papillomavirus type 16 infection;[26] however, the mechanism related to the involvement of IRF6 in the host anti-HSV-1 response has not been reported. Therefore, in the present study, we investigated the role of IRF6 in the development of HSV-1-induced HSK. We hypothesize that IRF6 exerts its antiviral effect by promoting IFN expression during HSV-1 infection and that RIPK4 and PKD regulate IRF6 expression.

Methods

Cells

Vero cells were purchased from the Shanghai Cell Bank, Chinese Academy of Sciences (ATCCCCL81). Complete Vero cell medium was prepared with 10% fetal bovine serum (Procell, Wuhan, China), 1% penicillin-streptomycin solution (Solarbio, Beijing, China), and 89% high-glucose DMEM (Procell, Wuhan, China). Mouse dendritic cells DC2.4 were purchased from Procell (Wuhan, China). Complete dendritic cell medium was prepared with 10% fetal bovine serum (Procell, Wuhan, China), 1% penicillin-streptomycin solution (Solarbio, Beijing, China), and 89% high-glucose DMEM (Procell, Wuhan, China). Human corneal epithelial cells (ZQ1003) were purchased from Shanghai Zhong Qiao Xin Zhou Biotechnology Co., Ltd. HCEC complete medium was prepared as follows: Dulbecco's modified Eagle's medium/nutrient mixture F-12 containing 10% fetal bovine serum (Procell, Wuhan, China), 5 U/mL recombinant human insulin, 10 ng/mL recombinant human epidermal growth factor and 1% penicillin-streptomycin solution. The cells were grown at 37 °C with 5% CO_2 in a humidified incubator.

Virus

Vero cells were used to resuspend the HSV-1 McKrae strain. Virus inoculation was performed when the cell density reached 90%. The virus solution was inoculated into Vero cells, which were then placed in a 37 °C incubator for 90 min. During the incubation period, the flask was shaken thoroughly every 15 min to ensure that the virus solution fully contacted the Vero cells. After 48 h of incubation, the supernatant was removed after centrifugation, and the virus solution was harvested and stored at −80 °C. The virus titer was $10^{5.8}$ $TCID_{50}$/mL before use. The configuration of the virus maintenance medium was 4% fetal bovine serum and 96% high-glucose DMEM.

Animals

BALB/c female mice were purchased from Skebes Biotechnology (Henan, China), selected to be 6–8 weeks old and weighing between 18 and 22 g. The mice were housed in an SPF environment and acclimated to the environment for one

week after arrival in the laboratory. The animal experiments were approved by the Ethics Committee of Shengjing Hospital of China Medical University (ethics number: 2023PS605K).

Animal Model

The mouse cornea was observed under a microscope, and it was confirmed that the cornea was smooth, complete, and transparent and that there was no trauma, redness, swelling, or foreign body in the eye. After isoflurane anesthesia, a 1 mL syringe needle was used to make a "#" shape scratch on the corneal epithelial layer of the mice, 5 μL of virus solution was added, and 5 μL of virus maintenance solution was added to the control group. The scratch depth was limited to the corneal epithelium and did not reach the stromal layer. The eyelids of the mice were gently pressed and kneaded to ensure that the liquid fully contacted the cornea. After modeling, the corneal lesions of the mice were observed under a microscope every d, and the clinical scores were recorded:[27] 0, intact epithelium (no lesion); 1, diffuse punctate lesions; 2, dendritic lesion occupying < 1/4 of the entire epithelial area; 3, severe dendritic lesion extending across > 1/4 of the entire epithelial area; 4, geographic lesion on the corneal epithelium; and 5, completely swollen eye. All procedures were performed with the animals under isoflurane anesthesia, and only one cornea from each mouse was infected. Euthanasia was performed using carbon dioxide inhalation.

Proteomics Detection

Label-free quantification was performed on corneal tissues from six groups of mice (three normal controls and three HSK groups; four corneas per group). Total protein was extracted, reduced, alkylated, quantified, and desalted. Peptides were diluted to 1 μg/μL, and 5 μL was injected for LC-MS/MS analysis using a Q-Exactive HFX mass spectrometer (Thermo Fisher Scientific). Chromatographic separation was achieved using a pre-column (300 μm × 0.5 mm, 3 μm) and an analytical column (75 μm × 150 mm, 3 μm, Welch). The mobile phases were: A (98% H□O, 2% ACN, 0.1% FA) and B (98% ACN, 2% H□O, 0.1% FA). MS1 scans were acquired at 60,000 resolution over 350–1500 m/z; MS2 at 15,000 resolution with NCE 28. Raw data were processed using MaxQuant (v1.6.15.0).

Total RNA Extraction and qPCR

Total RNA was extracted from the samples using TRIzol (Seven, China), and gDNA was removed from the total RNA using a reverse transcription kit followed by reverse transcription. qPCR was performed using SYBR Green (Takara) and a 7500 Fast Real-Time PCR Detection System (Applied Biosystems, Waltham, MA, USA). The sequences of the qPCR primers used are listed in Supplementary Table 1.

Total Protein Extraction and Western Blotting

The samples were lysed with RIPA lysis buffer (EpiZyme, Shanghai, China) and subjected to ultrasonic fragmentation. After centrifugation at 12,000 rpm for 25 min, the supernatant was removed to obtain the total protein solution. The protein sample concentration was determined by a BCA kit, and the samples were prepared to a uniform concentration. Loading buffer was added to the protein samples, which were then placed in a metal bath at 100 °C for heat denaturation. Protein samples were added to SDS–polyacrylamide gels for electrophoresis, and proteins were transferred to PVDF membranes. The PVDF membrane was blocked with rapid blocking solution at 25 °C for 30 min, incubated with the primary antibody at 4 °C overnight (Dilution ratio of the primary antibody was 1:1000, the antibody information is provided in Supplementary Table 2A), washed with TBST, and incubated with the secondary antibody (Dilution ratio 1:5000) at 25 °C for one h. After washing with TBST, the luminescent solution was added to the machine for detection. Gray value measurements were performed using ImageJ software.

Flow Cytometry

On the 14th d after infection, mouse spleens were collected, ground, made into single-cell suspensions, and centrifuged at 350 × *g* for 5 min, after which the supernatant was discarded. Live cells were counted and resuspended in a cell-staining buffer at a concentration of 5–10×10^6 cells/mL. Mouse splenocytes were resuspended in 2 mL of erythrocyte lysate and incubated for 15 min at room temperature in the dark. Then, 2 mL of phosphate-buffered saline (PBS) was added, the mixture was centrifuged at 350 × *g* for 5 min, and the supernatant was discarded. Then, 2 μL of flow fluorescent antibody

was added to 100 μL of cell suspension and incubated on ice for 20–30 min in the dark. Then, 250 μL of 1X TF Fix/Perm Buffer was added to each tube to resuspend the cell precipitate, which was subsequently centrifuged at 450 × *g* for 5 min, incubated with 1 mL of 1X TF Perm/Wash Buffer for 10 min, and centrifuged at 450 × *g* at 4 °C for 5 min. The fixed/permeabilized cells were subsequently resuspended in 100 μL of TF Perm/Wash Buffer, and the appropriate concentration of intranuclear fluorescent antibody was added, followed by vortexing and incubation at 4 °C for 40–45 min. The cells were subsequently washed twice with 1 mL of cell staining buffer and centrifuged at 450 × *g* for 5 min. The cells were subsequently resuspended in cell staining buffer (300 μL) and filtered through a 70-μm cell filter for on-board. Antibody information is detailed in Supplementary Table 2B. All the above reagents were purchased from BD Biosciences (USA).

Histopathology and Immunofluorescence Staining

The eyeballs of the mice were soaked in paraformaldehyde for at least 24h, dehydrated with increasing concentrations of alcohol, and permeabilized with xylene. The tissues were embedded in paraffin to make paraffin specimens, which were cut into paraffin sections with a thickness of 4 μm. Sections were stained with hematoxylin and eosin. The slices were sealed with neutral gum. Images were taken using a microscope (Nikon, E800,Japan).

For immunofluorescence staining, the paraffin sections were deparaffinized, antigen repair solution was used for antigen thermal repair, the sections were washed with PBS and incubated with blocking solution at room temperature for 30 min, the blocking solution was removed, the primary antibody was added (Multiple of dilution 1:200), the sections were incubated at 4 °C overnight, the sections were washed with PBS, a fluorescent secondary antibody (1:200, Fluorescent goat anti-rabbit IgG antibody and fluorescent goat anti-mouse IgG antibody, Absin, Shanghai, China) was added, the sections were incubated at 25 °C for 30 min, and the sections were washed with PBS. DAPI solution was added, and the sections were incubated at 25 °C for 5 min. The sections were washed with PBS, and the slides were sealed with an anti-fluorescence quenching solution (Seven, Beijing, China). The tissues were subsequently viewed under a confocal microscope (Zeiss, Germany).

Lentivirus siRNAs and Plasmids

Lentiviruses used in animals were purchased from GenePharma Biotech Company (Suzhou, China). The siRNAs and plasmids used in the cells were purchased from GenePharma Biotech Company (Suzhou, China) and GeneChem Co., Ltd. (Shanghai, China), respectively. The siRNA and plasmid transfections were performed using Lipofectamine 3000 transfection reagent (Thermo, USA). Sequence information is provided in Supplementary Table 3. Lentivirus injections were given every other d for one week before establishing the model. Lentivirus was administered to the animals at a dose of 5 μL/animal/d through subconjunctival injection for three injections before HSV-1 inoculation. The siRNA and plasmid doses were determined in a preexperiment. Transfection efficiency was measured using qPCR and Western blot.

Statistical Analyses

Statistical analysis of the experimental results was performed using GraphPad Prism software, and the data are expressed as the mean ± SD or mean ± SEM. Differences between groups were analyzed using Student's *t*-test, and $P < 0.05$ was considered to indicate statistical significance. All experiments were repeated three times independently.

Results

HSV-1 Infection Leads to Reduced IRF6 Expression

We established a primary infection model in mice. Mouse corneas were obtained at the onset of corneal stroma opacity and neovascularization on d 11 post-infection,[28,29] and proteomic analysis of mouse corneal tissues was performed. Considering the pathological mechanism of HSK, we focused on the IFN-related factor IRF6, which was abnormally downregulated. To verify this result, BALB/c mice were used to establish an HSK model and IRF6 expression levels in corneal tissues (Three corneal tissues were mixed as one group) were detected via Western blotting on d 1, 3, 5, 7, 14, and 21 post-infection (Figure 1A and B). HSV-1 virus solution was added to single-layer human corneal epithelial cells

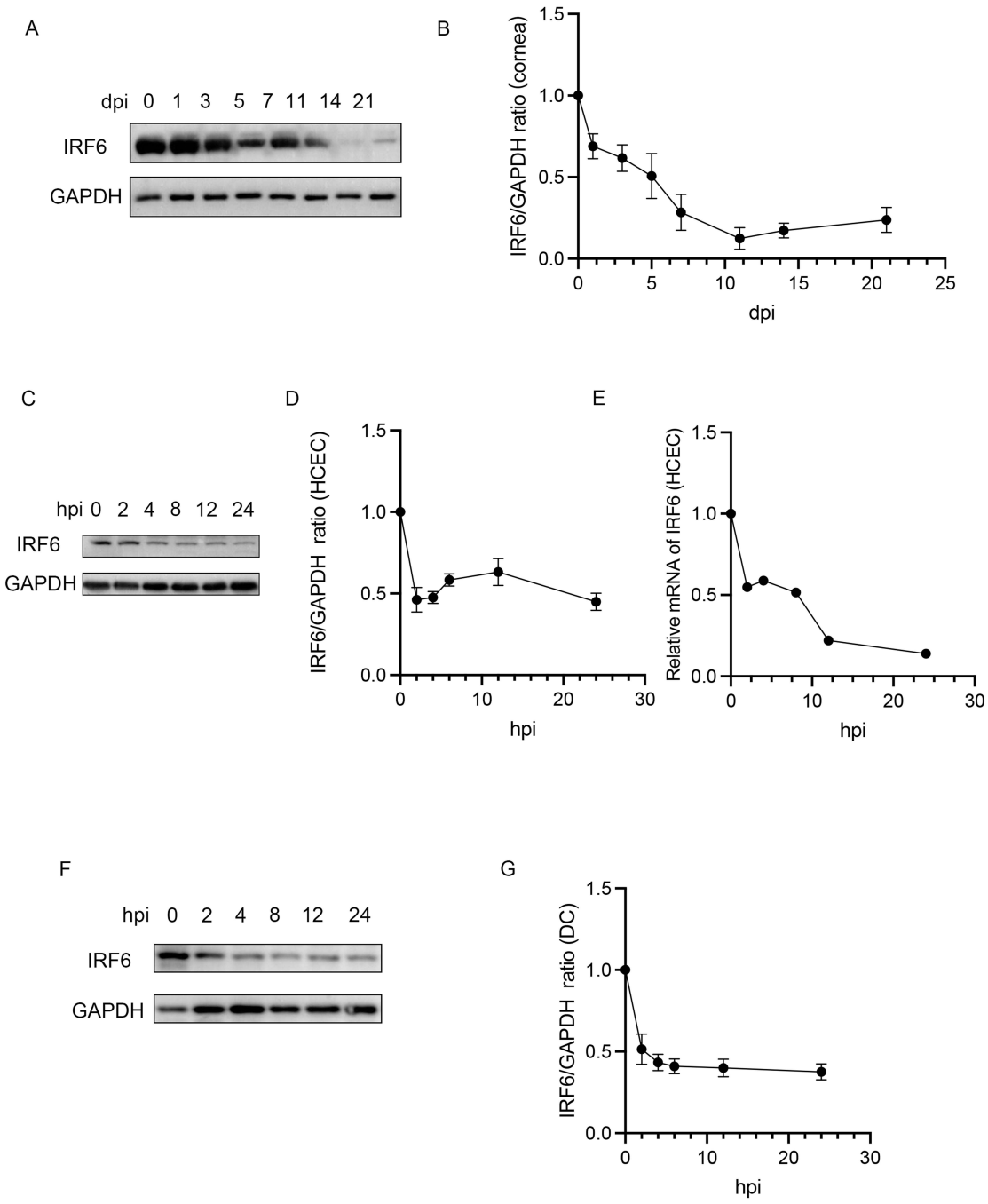

Figure 1 Herpes simplex virus 1 (HSV-1) infection downregulates IRF6 expression. (**A**) The right eyes of female BALB/c mice were inoculated with HSV-1, and mouse corneas were collected at 0, 1, 3, 5, 7, 11, 14, and 21 d after infection for detection of interferon regulatory factor 6 (IRF6) expression via Western blotting. (**B**) Grayscale statistical plots of changes in IRF6 expression in mouse corneas infected with HSV-1 using glyceraldehyde 3-phosphate dehydrogenase (GAPDH) as an internal reference; three corneas per group. The 0dpi group was used as the control group. The data are shown as the means ± SEMs of three independent experiments. (**C**) HSV-1 was inoculated into human corneal epithelial cells (HCECs) at a multiplicity of infection (MOI) of 10 and harvested at 0, 2, 4, 8, 12, and 24 h post-infection for detection of IRF6 expression via Western blotting. (**D**) Grayscale statistical graphs showing changes in IRF6 expression in HCECs infected with HSV-1; GAPDH was used as an internal reference. The 0hpi group was used as the control group. The data are shown as the means ± SEMs of three independent experiments. (**E**) HSV-1 was inoculated into HCECs at an MOI of 10, and the cells were harvested at 0, 2, 4, 8, 12, and 24 h post-infection to detect changes in IRF6 mRNA expression via quantitative PCR (qPCR) with GAPDH as an internal reference. The data are shown as the means ± SEMs of three independent experiments. (**F**) Mouse dendritic cells were inoculated with HSV-1 at an MOI of 10, and the cells were harvested at 0, 2, 4, 8, 12, and 24 h post-infection for detection of IRF6 expression via Western blotting. (**G**) Grayscale statistical plots of changes in IRF6 expression after dendritic cell infection with HSV-1 using GAPDH as an internal reference. The data are shown as the means ± SEMs of three independent experiments.

Abbreviations: dpi, d post-infection; hpi, h post-infection.

https://doi.org/10.2147/JIR.S526580

and mouse dendritic cells to achieve a multiplicity of infection (MOI) of 10, respectively. Infected cells were harvested at multiple time points post-infection to extract total proteins and RNA, and changes in IRF6 expression levels were detected via Western blotting and quantitative PCR (Figure 1C–F). HSV-1 infection triggered a decrease in IRF6 expression in corneal tissues and HCECs. The IRF6 expression level decreased from the first d after HSV-1 infection in mouse corneas until the 21st d after infection (Figure 1B). IRF6 expression in human corneal epithelial cells (Figure 1D and E) and mouse dendritic cells (Figure 1G) decreased continuously 2 h after HSV-1 infection until 24 h post-infection.

IRF6 Inhibits HSV-1 Replication in HCECs

Small interfering RNA (siRNA) was used to silence the expression of IRF6 in HCECs, and an overexpression plasmid was used to overexpress IRF6 in HCECs to investigate the effect of IRF6 on HSV-1 replication; the silencing efficiencies were confirmed using qPCR and Western blotting (Figure 2A and B). HSV-1 was inoculated into transfected HCECs at an MOI of 10. The cells were harvested at 24 h after infection for the qPCR assay, which showed that the expression of the HSV-1 replication-related genes *gD* and *VP16* was elevated in the IRF6-silenced group and downregulated in the IRF6-overexpressing group compared to the control group, suggesting that IRF6 suppressed the transcription of HSV-1 proliferation-related genes, thus inhibiting viral replication (Figure 2C). The virus titers of the cell culture supernatant of the above groups were detected at the same time, and the results were consistent with the above experiments (Figure 2D). IRF family members all possess a highly conserved N-terminal helix-turn-helix DNA-binding domain and a less conserved C-terminal protein-binding domain.[19] The structural domain of IRF6 may activate the expression of IFN-related genes.[13] To explore this function, we examined the expression of IFN-related genes in the above samples; the transcript levels of IFN-β, ubiquitin-like protein ISG15 (ISG15), and IFN-induced protein with tetratricopeptide repeat 1 (IFIT1) were increased in the IRF6 overexpression group compared with those in the control group (Figure 2E).

IRF6 Overexpression Inhibits HSV-1 Replication in Mouse Corneas

Because IRF6 was expressed at low levels after infection, we investigated whether elevated IRF6 expression could affect the extent of HSK in BALB/c mice. Lentiviral transfection was used to overexpress IRF6 locally in mouse corneas. Lentiviruses overexpressing IRF6 were injected into the subconjunctiva of the right eye. One injection was administered every 2 d, for a total of three injections, and the second d after the last injection was recorded as d 0. The injected corneal tissues were collected (Three corneal tissues were mixed as one group), and total protein was extracted after lysis on d 14 to test the expression level of IRF6 (Figure 3A). Western blotting revealed that IRF6 was more highly expressed in the overexpression group than in the lentiviral control group (Figure 3B). An HSK model was established using lentivirus-pretreated mice. On the 14th d after infection, corneas were collected for Western blotting, and paraffin sections of mouse eyes were obtained for immunofluorescence assays. The expression levels of the HSV-1 replication-associated proteins infected cell protein 0 (ICP0), glycoprotein D (gD), virion protein 16 (VP16), and HSV-1 DNA polymerase UL42 decreased in the corneas of mice in the IRF6 overexpression group compared to those in the lentiviral control group (Figure 3C and D). Immunofluorescence revealed that the level of red fluorescence, representing the HSV-1 surface glycoprotein gD, was lower in the corneas of mice overexpressing IRF6 than in those of the lentiviral control group. In contrast, green fluorescence, representing IRF6 expression, was increased (Figure 3E and F). These results indicate that overexpressing IRF6 in mouse corneas can effectively reduce HSV-1 replication.

IRF6 Overexpression in Mouse Corneas Reduces HSK Severity

Lentivirus was used to over-express IRF6 in mouse cornea, and subsequently a mouse model of HSK was established. Pathological scores on d 0–14 post-infection showed that the severity of corneal inflammation in mice with IRF6 overexpression was attenuated compared with that in the control group (Figure 4A). Compared with the lentivirus control group, the tear virus titer of IRF6 overexpression group was decreased (Figure 4B). On the 14th d after infection, photographs of the external eyes of the mice were captured. The eyeballs of the mice were stained with hematoxylin and eosin (Figure 4C). On the 14th d after infection, the corneal epithelial cells of the mice in the lentiviral control group were abnormally proliferated and arranged disorderly, with many inflammatory cells infiltrating the stroma. The collagen

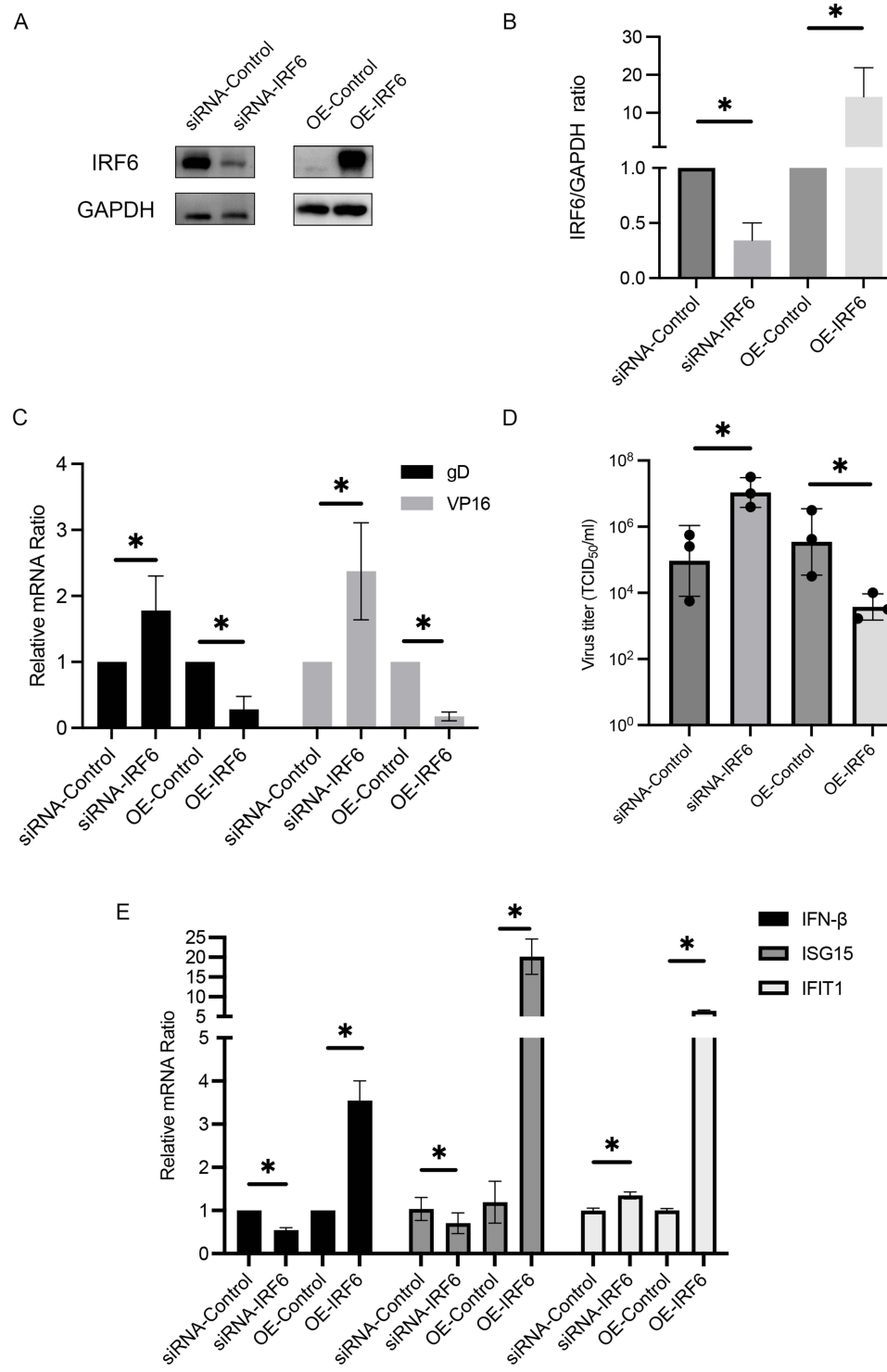

Figure 2 Inhibition of HSV-1 replication by IRF6 in HCECs. (**A**) Expression of IRF6 in HCECs was determined using Western blotting 24 h after transfection with small interfering RNAs (siRNAs) and plasmids. (**B**) Relative gray value statistics using GAPDH as an internal reference. The transfection efficiency was as expected. The data are expressed as the means ± SDs of three independent experiments; *p < 0.05 (n=3). (**C**) HSV-1 was inoculated into HCECs after transfection with siRNA and plasmids, and the cells were harvested at 24 h post-infection for total RNA extraction to detect HSV-1 gD and VP16 expression. The data are expressed as the means ± SDs of three independent experiments; *p < 0.05 (n=3). (**D**) HSV-1 was inoculated into HCECs after transfection with siRNA and plasmids, viral titers were measured in cell culture supernatants 24h after infection. The data are expressed as the means ± SDs of three independent experiments; *p < 0.05 (n=3). (**E**) HSV-1 was inoculated into HCECs after transfection with siRNA and plasmids, and the cells were harvested at 24 h post-infection for total RNA extraction to detect the levels of the interferon (IFN)-related genes IFN-β, IFN-stimulated gene 15 (ISG15), and IFN-induced protein with tetratricopeptide repeats 1 (IFIT1). The data are expressed as the means ± SDs of three independent experiments; *p < 0.05 (n=3).

https://doi.org/10.2147/JIR.S526580

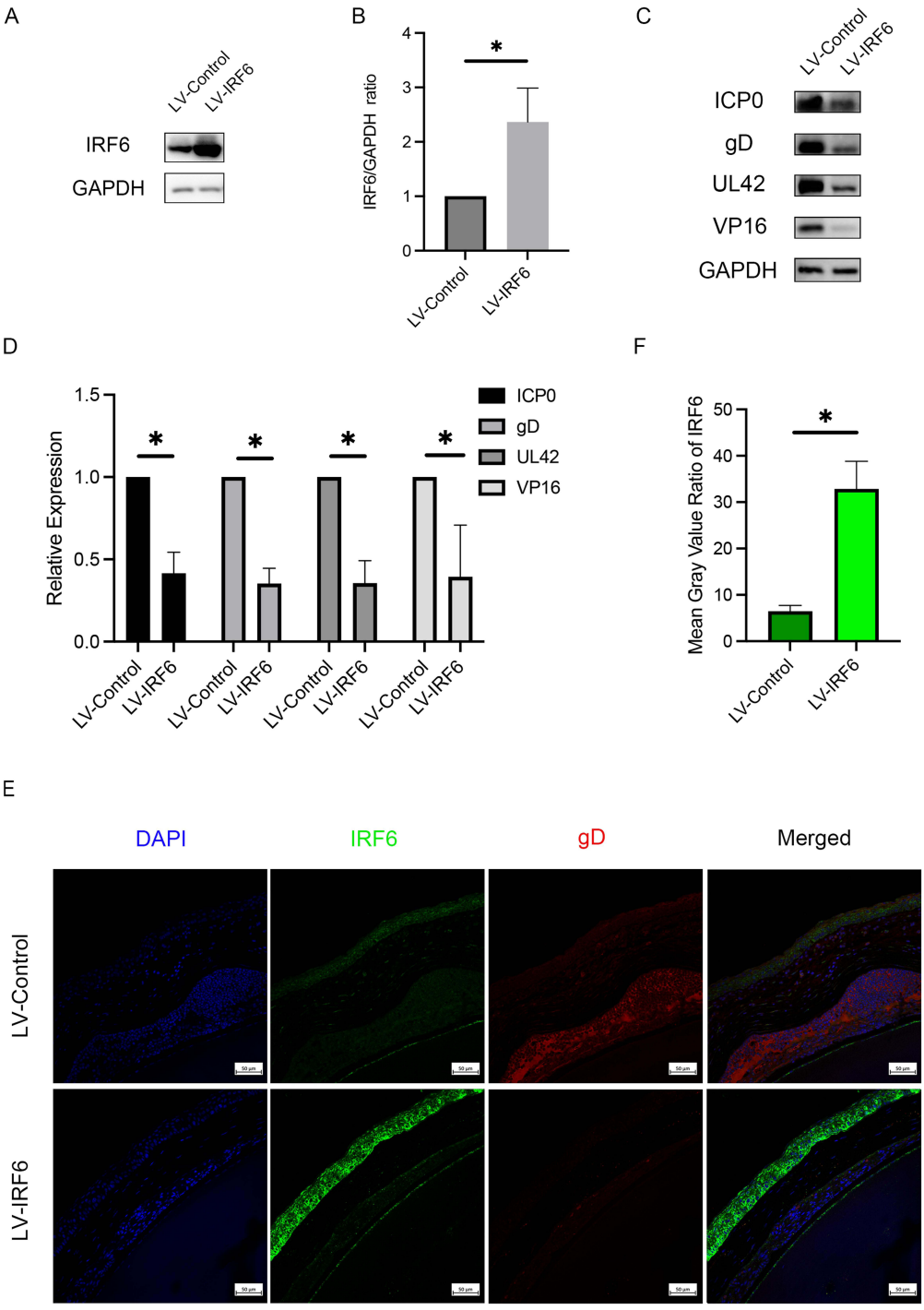

Figure 3 Inhibition of HSV-1 replication by overexpressing IRF6 in mouse corneas. (**A**) Lentivirus was injected under the bulbar conjunctiva, and IRF6 was overexpressed locally in the right cornea of mice. The control group was injected with a lentiviral control reagent, and the second d after the last injection was recorded as d 0. The right cornea of each mouse was harvested on d 14 for Western blotting. (**B**) Grayscale statistical plots of changes in IRF6 expression in mouse corneas after lentiviral treatment using GAPDH as an internal reference; three corneas in each group. The data are shown as the means ± SDs of three independent experiments; *$p < 0.05$ (n=3). (**C**) IRF6 was overexpressed in the right cornea of mice infected with lentivirus and inoculated with HSV-1 on the d after the last injection. The corneas of the mice were collected on d 14 post-infection for Western blotting. (**D**) Grayscale statistical plots of changes in HSV-1-related protein expression in the corneas of mice overexpressing IRF6 infected with HSV-1 14 d after infection, with GAPDH serving as an internal reference; three corneas from each group are shown. The data are shown as the means ± SDs of three independent experiments; *$p < 0.05$ (n=3). (**E**) The corneas of IRF6-overexpressing mice infected with HSV-1 14 d after infection were collected from the right eyeballs of the mice, paraffin sectioned, and stained for immunofluorescence. Blue fluorescence represents the nucleus of the cell, green fluorescence represents IRF6, and red fluorescence represents HSV-1 gD. Magnification 100×, scale bar: 50μm. (**F**) Mean Gray Value Ratio of IRF6. The data are shown as the means ± SDs of three independent experiments; *$p < 0.05$ (n=3).

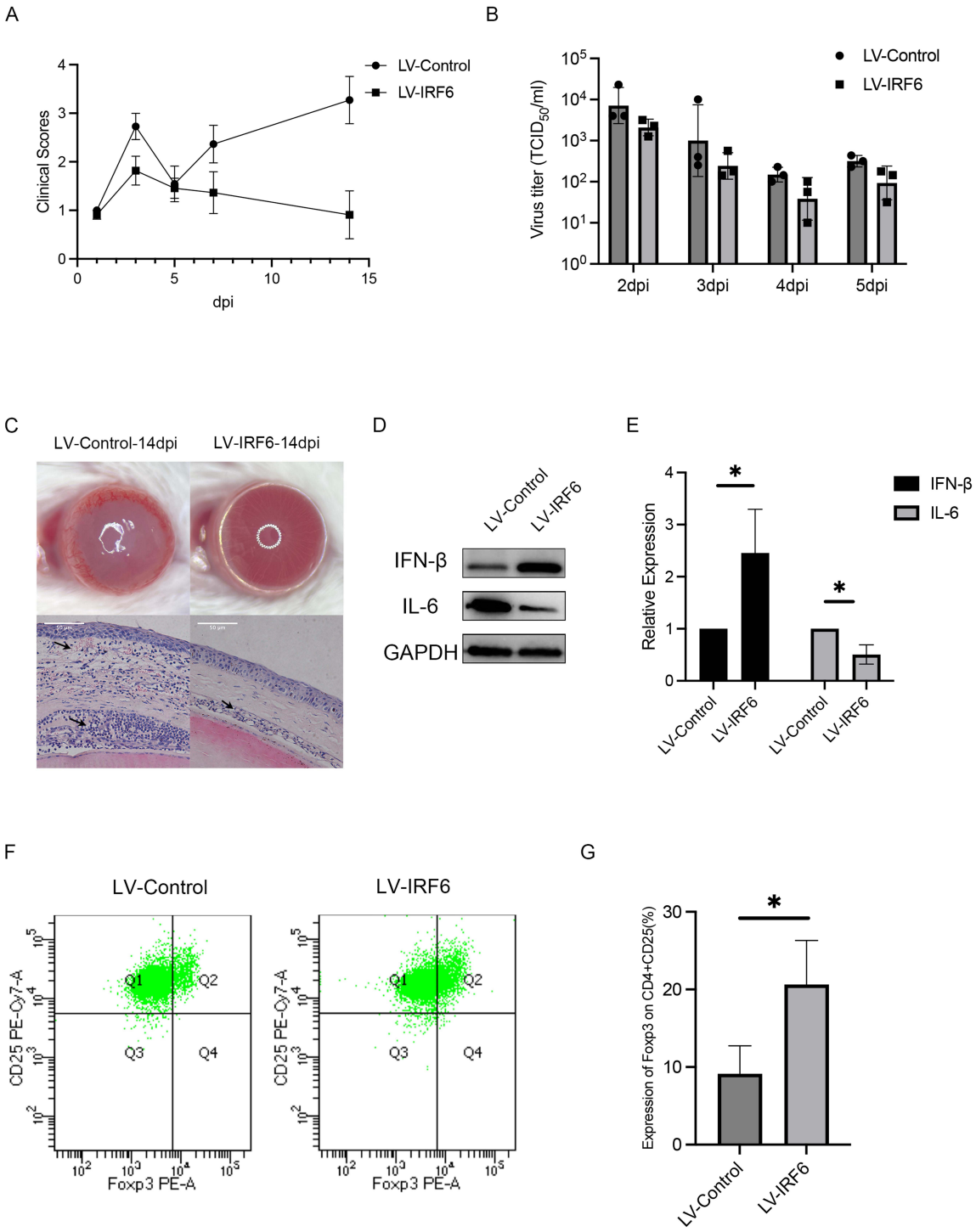

Figure 4 Overexpressing IRF6 in mouse corneas alleviates HSK severity. (**A**) Statistical graph of the clinical scores of lentiviral-overexpressing IRF6 mice 0–14 d after corneal infection with HSV-1; eleven mice per group. The data are shown as the mean ± SEM of three independent experiments. (**B**) Lentivirus-overexpressing IRF6 mice were infected with HSV-1, and viral titers in tears were measured 2, 3, 4, and 5 days after infection. The data are shown as the mean ± SEM of three independent experiments. (**C**) Photographs of the outer eyes of mice with lentiviral overexpression of IRF6 14 d after corneal infection with HSV-1 and hematoxylin and eosin-stained images of paraffin sections of mouse eyes. Arrows show inflammatory infiltration or RBCs in neovascularization (control) and only inflammatory cells (overexpression). Magnification 100×, scale bar 100 μm. (**D**) Overexpression of IRF6 in the right cornea of mice via lentivirus, inoculation with HSV-1 on the d after the last injection, and collection of mouse corneas for Western blotting on d 14 post-infection. (**E**) Grayscale statistical plots of changes in IFN-β and interleukin (IL)-6 expression in the corneas of IRF6-overexpressing mice infected with HSV-1 for 14 d; GAPDH was used as an internal reference, and three corneas from each group were used. The data are shown as the mean ± SD of three independent experiments; *p < 0.05 (n=3). (**F**) Spleens of lentivirus-overexpressing IRF6 mouse were harvested 14 d after HSV-1 infection, and the percentage of $CD4^+CD25^+FOXP3^+$ regulatory T cells (Tregs) was detected using flow cytometry. (**G**) Statistical histogram of the percentage of $CD4^+CD25^+FOXP3^+$ Tregs. The data are shown as the mean ± SD of three independent experiments; *p < 0.05 (n=3).

https://doi.org/10.2147/JIR.S526580

fibers in the stroma were loosely disorganized, and many inflammatory cells infiltrated the corneal endothelium. In the overexpression group, only a small number of corneal epithelial cells proliferated, and inflammatory cell infiltration in the stromal layer decreased (Figure 4C). Western blotting was performed on the corneas of the mice 14 d after infection (Three corneal tissues were mixed as one group). The expression of the anti-inflammatory cytokine IFN-β increased. However, the expression of the proinflammatory cytokine IL-6 decreased in the IRF6-overexpressing group compared with the control group, suggesting that IRF6 overexpression in the corneas of the mice inhibited the increase in inflammation (Figure 4D and E). Fourteen d after infection, the spleens of the mice were collected, and the percentage of $CD4^+CD25^+FOXP3^+$ regulatory T cells (Tregs) in the spleens was detected using flow cytometry (Figure 4F), which revealed that the percentage of Tregs was elevated in the IRF6-overexpressing group (Figure 4G). This result indicates that IRF6 overexpression inhibits the progression of inflammation to some extent.

IRF6 Phosphorylation is Influenced by RIPK4 and PKD During Infection

Proteomic assays performed earlier in our project revealed that PKD was highly expressed in the corneal tissues of mice 11 d after infection. Therefore, to investigate whether RIPK4 and PKD are involved in IRF6 phosphorylation during HSV-1 infection, we silenced and overexpressed RIPK4 and PKD in HCECs using siRNA and plasmids, confirmed the silencing and overexpression efficiency (Figure 5A and B), and then inoculated the cells with HSV-1 at an MOI of 10. The cells were harvested at 24 h post-infection to extract total protein for Western blotting (Figure 5C). When p-IRF6/IRF6 was used to represent the degree of IRF6 phosphorylation, the p-IRF6/IRF6 ratio decreased in the siRNA-PKD group, and the p-IRF6/IRF6 ratio decreased in the siRNA-RIPK4 group (Figure 5D). The IRF6 expression level was elevated in the siRNA-PKD and siRNA-RIPK4 groups compared with that in the control group (Figure 5E and F). These findings suggest that RIPK4 and PKD are involved in IRF6 phosphorylation during HSV-1 infection. Silencing RIPK4 and PKD decreased the phosphorylation level of IRF6, thereby reducing the degradation of IRF6 induced by phosphorylation.

Discussion

The innate immune response is the first line of host defense against viral invasion. Intracellular receptors immediately recognize viral nucleic acids to activate antiviral immune responses upon HSV-1 invasion. IFN triggers the defense of the immune system and effectively inhibits viral replication.[30] dsDNA, dsRNA, and glycoproteins produced during viral replication are recognized by multiple cytoplasmic sensors, triggering an antiviral immune response in the host cell. Furthermore, the activation of the cGAS/STING and TLR3/TRIF pathways contributes to the IFN response by inhibiting viral replication.[31] Recently, new advances have been made in the research on HSK, and studying these mechanisms has laid the foundation for identifying effective targets to treat HSK. HSV-1-erasing lentiviral particles were utilized to impede viral replication both at the site of infection and within the latent reservoir,[11] and the clinical treatment based on this research has also been proven to be effective.[32] Therefore, effectively controlling viral replication during the early stages of infection and preventing virus-triggered hyperimmune responses are top priorities. Viruses interfere with intracellular signaling by promoting the synthesis of multiple enzymes, and ICP0 expressed by HSV-1 can block the STING/IRF3 signaling pathway in a variety of ways and suppress innate immunity, thereby evading the immune system.[33,34] The type I IFN response plays a decisive role by inhibiting viral replication and controlling infection.[35] In the subsequent stage of adaptive immunity, many immune cells infiltrate the cornea, primarily through the release of corresponding cytokines from $CD4^+$ T cells.[27] However, excessive immune responses damage innate corneal cells and cause irreversible changes in corneal tissue structure.[36] Treg cells can reduce the severity of corneal inflammation,[37] and Treg cells inhibit the occurrence of an excessive immune response by controlling the release of inflammatory cells and chemokines and have a positive effect on the prognosis of HSK patients.[38]

In clinical treatment, glucocorticoid drugs are often along with antiviral agents to suppress the immune response and reduce corneal edema and scar formation. Nucleoside analogs such as ganciclovir and acyclovir are also the first choice for the treatment of HSK.[39] However, long-term use leads to the development of drug resistance in viral strains and an increase in the frequency of viral recurrence. Furthermore, the severity of corneal inflammatory damage worsens with each recurrence, ultimately leading to irreversible vision loss.[40] Therefore, modulating the antiviral effects of the body's innate immune

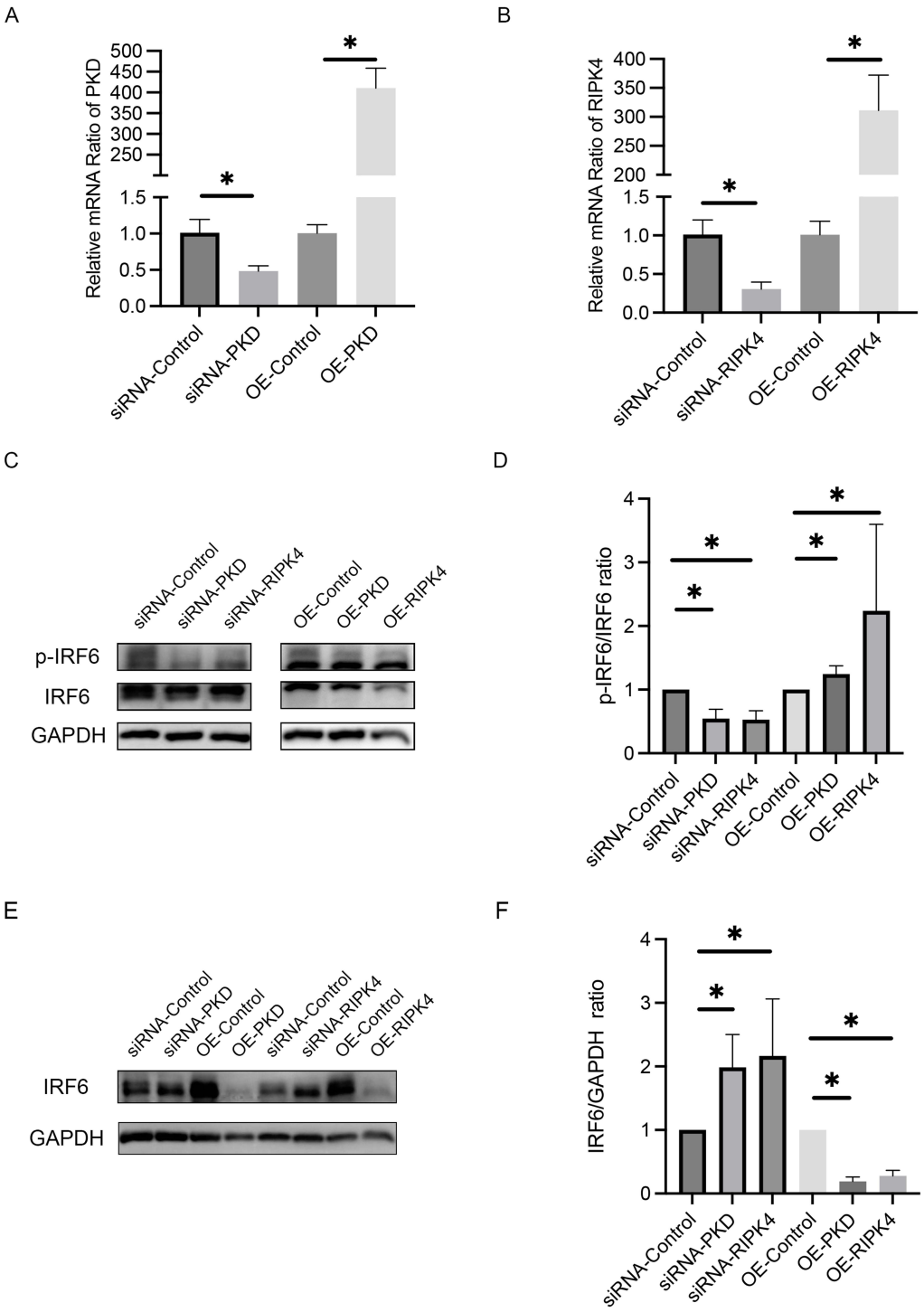

Figure 5 Effect of protein kinase C delta (PKD) and receptor-interacting protein kinase 4 (RIPK4) on IRF6 phosphorylation. (**A**) Silencing and overexpression of PKD in HCECs were performed using siRNA and plasmids. Transfection efficiency was measured using qPCR. The data are shown as the mean ± SD of three independent experiments; *p < 0.05 (n=3). (**B**) Silencing and overexpression of RIPK4 in HCECs were performed using siRNAs and plasmids. Transfection efficiency was measured using qPCR. The data are shown as the mean ± SD of three independent experiments; *p < 0.05 (n=3). (**C**) Silencing and overexpression of PKD and RIPK4 in HCECs were performed using siRNAs and plasmids. The cells were inoculated with HSV-1 at an MOI of 10, the cells were harvested 24 h post-infection, and changes in IRF6 and p-IRF6 expression were detected via Western blotting. (**D**) Statistical graph of the p-IRF6/IRF6 grayscale ratio. The data are shown as the mean ± SD of three independent experiments; *p < 0.05 (n=3). (**E**) Silencing and overexpression of PKD and RIPK4 in HCECs were performed using siRNAs and plasmids. The cells were inoculated with HSV-1 at an MOI of 10, the cells were harvested 24 h post-infection, and changes in IRF6 expression were detected via Western blotting. (**F**) Grayscale statistical plots of IRF6 expression levels detected using Western blotting with GAPDH as an internal reference. The data are shown as the mean ± SD of three independent experiments; *p < 0.05 (n=3).

https://doi.org/10.2147/JIR.S526580

response, especially the IFN response, and inhibiting the damage to corneal tissues caused by early viral replication and the excessive adaptive immune response induced by viral antigens are the targets of future investigations.[41,42]

In the present study, IRF6 was downregulated in the corneas of HSK model mice, and the antiviral effects of IRF6 were demonstrated in animal and cellular studies. In contrast, PKD expression was high in the corneal tissues of HSK mice. Previous studies have shown that IRF6 differentially regulates Toll-like receptor 2-mediated chemokine gene expression in epithelial cells;[43] IRF6 is highly expressed in keratinocytes and selectively regulates the direction of the response to TLR3.[44] IRF family proteins generally exert physiological effects through phosphorylation and dimer formation.[45] Phosphorylation regulates the activity and stability of IRF6. Furthermore, RIPK4 directly regulates IRF6 transactivator activity and nuclear translocation during keratinocyte growth and differentiation, and PKD is involved in intracellular phosphorylation during HSV-1 infection.[46] Gene promoter reporter assays have shown that PKC activation induces IRF6 activity.[24] PKD then forms a complex with RIPK4, which in turn affects IRF6 activity.[47,48] Although MyD88 and TBK1 phosphorylate IRF6 in zebrafish cells, the effect of phosphorylation on its function and stability at different sites of human IRF6 has not been explored.[49]

Because IRF6 is expressed at low levels during HSV-1 infection, we silenced and overexpressed IRF6 in human corneal epithelial cells and inoculated these cells with HSV-1. Moreover, HSV-1 replication was significantly inhibited by IRF6 overexpression, and the transcript levels of the key products of viral replication, the HSV-1 capsid protein VP16 and glycoprotein gD,[50] were reduced. In contrast, the transcript levels of the antiviral factor IFN-β and the IFN-related genes ISG15 and IFIT1 were elevated.[51,52] Furthermore, local IRF6 overexpression in mouse corneas effectively inhibited viral replication and alleviated the severity of HSK by promoting the expression of the inhibitory viral replicative cytokine IFN-β and inhibiting the expression of the proinflammatory cytokine IL-6. Silencing of PKD and RIPK4 in HCECs and inoculation with HSV-1 indicated that PKD and RIPK4 were involved in IRF6 phosphorylation and affected its degradation during infection.[53,54]

The limitations of this study were that the silencing and overexpression of the target genes by existing means are far less effective than those in gene-edited mice. Additionally, the time points at which HSK mice were sampled after lentiviral infection were few and failed to reflect the role played by IRF6 during the entire HSV-1 infection process. More effective technical means of intervention should be used in future studies, and the reasons for the downregulation of IRF6 and the relationship between IRF6 and TLRs during HSV-1 infection require further exploration.

Conclusion

In conclusion, this study is the first to illustrate the role of IRF6 in HSV-1 infection. IRF6 inhibits viral replication and alleviates HSK severity by promoting IFN-β expression and suppressing IL-6 expression. PKD and RIPK4 were involved in IRF6 phosphorylation during infection. The results of our study indicate that the use of IRF6 is a potential therapeutic strategy for treating HSV-1-induced HSK.

Data Sharing Statement

The authors confirm that the data supporting the findings of this study are available within the article.

Ethics Statement

This study was reviewed and approved by the Ethics Committee of Shengjing Hospital, Affiliated with China Medical University (ethics number: 2023PS605K).

All experiments adhered to the ARVO statement for the Use of Animals in Ophthalmic and Vision Research.

Acknowledgments

This project was funded by the Department of Science and Technology of Liaoning Province (No. 2022JH2/101300044).

Disclosure

There are no conflicts of interest involved in this project.

References

1. Sun G, Kropp KA, Kirchner M, et al. Herpes simplex virus type 1 modifies the protein composition of extracellular vesicles to promote neurite outgrowth and neuroinfection. *mBio*. 2024;15(2):e0330823. doi:10.1128/mbio.03308-23
2. Kong E, Hua T, Li J, et al. HSV-1 reactivation results in post-herpetic neuralgia by upregulating Prmt6 and inhibiting cGAS-STING. *Brain*. 2024;15. doi:10.1093/brain/awae053
3. Liesegang TJ. Herpes simplex virus epidemiology and ocular importance. *Cornea*. 2001;20(1):1–13. doi:10.1097/00003226-200101000-00001
4. Farooq AV, Shukla D. Herpes simplex epithelial and stromal keratitis: an epidemiologic update. *Surv Ophthalmol*. 2012;57(5):448–462. doi:10.1016/j.survophthal.2012.01.005
5. James C, Harfouche M, Welton NJ, et al. Herpes simplex virus: global infection prevalence and incidence estimates, 2016. *Bull World Health Organ*. 2020;98(5):315–329. doi:10.2471/blt.19.237149
6. Krakowiak PA, Flores ME, Cuddy SR, et al. Co-option of mitochondrial nucleic acid-sensing pathways by HSV-1 UL12.5 for reactivation from latent infection. *Proc Natl Acad Sci U S A*. 2025;122(4):e2413965122. doi:10.1073/pnas.2413965122
7. Rowe AM, St Leger AJ, Jeon S, Dhaliwal DK, Knickelbein JE, Hendricks RL. Herpes keratitis. *Prog Retin Eye Res*. 2013;32:88–101. doi:10.1016/j.preteyeres.2012.08.002
8. Rousseau A, Pharm SB, Gueudry J, et al. Acyclovir-resistant Herpes Simplex Virus 1 keratitis: a Concerning and emerging clinical challenge. *Am J Ophthalmol*. 2022;238:110–119. doi:10.1016/j.ajo.2022.01.010
9. Awasthi S, Hook LM, Pardi N, et al. Nucleoside-modified mRNA encoding HSV-2 glycoproteins C, D, and E prevents clinical and subclinical genital herpes. *Sci Immunol*. 2019;4(39). doi:10.1126/sciimmunol.aaw7083
10. Bolland S, Pierce SK. Ups and downs in the search for a Herpes simplex virus vaccine. *Elife*. 2015;4. doi:10.7554/eLife.06883
11. Yin D, Ling S, Wang D, et al. Targeting herpes simplex virus with CRISPR-Cas9 cures herpetic stromal keratitis in mice. *Nat Biotechnol*. 2021;39(5):567–577. doi:10.1038/s41587-020-00781-8
12. Tamura T, Yanai H, Savitsky D, Taniguchi T. The IRF family transcription factors in immunity and oncogenesis. *Annu Rev Immunol*. 2008;26:535–584. doi:10.1146/annurev.immunol.26.021607.090400
13. Taniguchi T, Ogasawara K, Takaoka A, Tanaka N. IRF family of transcription factors as regulators of host defense. *Annu Rev Immunol*. 2001;19:623–655. doi:10.1146/annurev.immunol.19.1.623
14. Savitsky D, Tamura T, Yanai H, Taniguchi T. Regulation of immunity and oncogenesis by the IRF transcription factor family. *Cancer Immunol Immunother*. 2010;59(4):489–510. doi:10.1007/s00262-009-0804-6
15. Takaoka A, Tamura T, Taniguchi T. Interferon regulatory factor family of transcription factors and regulation of oncogenesis. *Cancer Sci*. 2008;99(3):467–478. doi:10.1111/j.1349-7006.2007.00720.x
16. Battistini A. Interferon regulatory factors in hematopoietic cell differentiation and immune regulation. *J Interferon Cytokine Res*. 2009;29(12):765–780. doi:10.1089/jir.2009.0030
17. Jefferies CA. Regulating IRFs in IFN driven disease. *Front Immunol*. 2019;10:325. doi:10.3389/fimmu.2019.00325
18. Wang H, Li W, Zheng SJ. Advances on innate immune evasion by avian immunosuppressive viruses. *Front Immunol*. 2022;13:901913. doi:10.3389/fimmu.2022.901913
19. Ma J, Chen J, Cui J, et al. A molluscan IRF interacts with IKKα/β family protein and modulates NF-κB and MAPK activity. *Int J Biol Macromol*. 2024;256(Pt 1):128319. doi:10.1016/j.ijbiomac.2023.128319
20. Oberbeck N, Pham VC, Webster JD, et al. The RIPK4-IRF6 signalling axis safeguards epidermal differentiation and barrier function. *Nature*. 2019;574(7777):249–253. doi:10.1038/s41586-019-1615-3
21. Bailey CM, Abbott DE, Margaryan NV, Khalkhali-Ellis Z, Hendrix MJ. Interferon regulatory factor 6 promotes cell cycle arrest and is regulated by the proteasome in a cell cycle-dependent manner. *Mol Cell Biol*. 2008;28(7):2235–2243. doi:10.1128/mcb.01866-07
22. De Groote P, Tran HT, Fransen M, et al. A novel RIPK4-IRF6 connection is required to prevent epithelial fusions characteristic for popliteal pterygium syndromes. *Cell Death Differ*. 2015;22(6):1012–1024. doi:10.1038/cdd.2014.191
23. Xu J, Wei Q, He Z. Insight into the function of RIPK4 in keratinocyte differentiation and carcinogenesis. *Front Oncol*. 2020;10:1562. doi:10.3389/fonc.2020.01562
24. Kwa MQ, Huynh J, Aw J, et al. Receptor-interacting protein kinase 4 and interferon regulatory factor 6 function as a signaling axis to regulate keratinocyte differentiation. *J Biol Chem*. 2014;289(45):31077–31087. doi:10.1074/jbc.M114.589382
25. Kwa MQ, Scholz GM, Reynolds EC. RIPK4 activates an IRF6-mediated proinflammatory cytokine response in keratinocytes. *Cytokine*. 2016;83:19–26. doi:10.1016/j.cyto.2016.03.005
26. Ainouze M, Rochefort P, Parroche P, et al. Human papillomavirus type 16 antagonizes IRF6 regulation of IL-1β. *PLoS Pathog*. 2018;14(8):e1007158. doi:10.1371/journal.ppat.1007158
27. Chen D, Liu Y, Zhang F, et al. 6-Thioguanine inhibits Herpes Simplex Virus 1 infection of eyes. *Microbiol Spectr*. 2021;9(3):e0064621. doi:10.1128/Spectrum.00646-21
28. Zhu S, Viejo-Borbolla A. Pathogenesis and virulence of herpes simplex virus. *Virulence*. 2021;12(1):2670–2702. doi:10.1080/21505594.2021.1982373
29. Yan C, Luo Z, Li W, et al. Disturbed Yin-Yang balance: stress increases the susceptibility to primary and recurrent infections of herpes simplex virus type 1. *Acta Pharm Sin B*. 2020;10(3):383–398. doi:10.1016/j.apsb.2019.06.005
30. Schumann T, Ramon SC, Schubert N, et al. Deficiency for SAMHD1 activates MDA5 in a cGAS/STING-dependent manner. *J Exp Med*. 2023;220(1). doi:10.1084/jem.20220829
31. Zheng C. Evasion of cytosolic DNA-stimulated innate immune responses by Herpes Simplex Virus 1. *J Virol*. 2018;92(6). doi:10.1128/jvi.00099-17
32. Wei A, Yin D, Zhai Z, et al. In vivo CRISPR gene editing in patients with herpetic stromal keratitis. *Mol Ther*. 2023;31(11):3163–3175. doi:10.1016/j.ymthe.2023.08.021
33. Harrell TL, Davido DJ, Bertke AS. Herpes Simplex Virus 1 (HSV-1) Infected Cell Protein 0 (ICP0) targets of ubiquitination during productive infection of primary adult sensory neurons. *Int J Mol Sci*. 2023;24(3):2931. doi:10.3390/ijms24032931
34. Tognarelli EI, Palomino TF, Corrales N, Bueno SM, Kalergis AM, González PA. Herpes Simplex Virus evasion of early host antiviral responses. *Front Cell Infect Microbiol*. 2019;9:127. doi:10.3389/fcimb.2019.00127

35. Zhu H, Zhang R, Yi L, Tang YD, Zheng C. UNC93B1 attenuates the cGAS-STING signaling pathway by targeting STING for autophagy-lysosome degradation. *J Med Virol*. 2022;94(9):4490–4501. doi:10.1002/jmv.27860
36. Setia M, Suvas PK, Rana M, Chakraborty A, Suvas S. Differential homing of monocytes and neutrophils in the epithelial layer of HSV-1 infected cornea regulates viral dissemination and wound healing. *Ocul Surf*. 2025;36:69–82. doi:10.1016/j.jtos.2025.01.002
37. Suvas S, Azkur AK, Kim BS, Kumaraguru U, Rouse BT. CD4+CD25+ regulatory T cells control the severity of viral immunoinflammatory lesions. *J Immunol*. 2004;172(7):4123–4132. doi:10.4049/jimmunol.172.7.4123
38. Veiga-Parga T, Suryawanshi A, Mulik S, et al. On the role of regulatory T cells during viral-induced inflammatory lesions. *J Immunol*. 2012;189 (12):5924–5933. doi:10.4049/jimmunol.1202322
39. Duxfield L, Sultana R, Wang R, et al. Ocular delivery systems for topical application of anti-infective agents. *Drug Dev Ind Pharm*. 2016;42 (1):1–11. doi:10.3109/03639045.2015.1070171
40. Lobo AM, Agelidis AM, Shukla D. Pathogenesis of herpes simplex keratitis: the host cell response and ocular surface sequelae to infection and inflammation. *Ocul Surf*. 2019;17(1):40–49. doi:10.1016/j.jtos.2018.10.002
41. Fu Y, Zhan X, You X, et al. USP12 promotes antiviral responses by deubiquitinating and stabilizing IFI16. *PLoS Pathog*. 2023;19(7):e1011480. doi:10.1371/journal.ppat.1011480
42. Liu Y, Xu XQ, Li WJ, et al. Cytosolic DNA sensors activation of human astrocytes inhibits herpes simplex virus through IRF1 induction. *Front Cell Infect Microbiol*. 2024;14:1383811. doi:10.3389/fcimb.2024.1383811
43. Kwa MQ, Nguyen T, Huynh J, et al. Interferon regulatory factor 6 differentially regulates Toll-like receptor 2-dependent chemokine gene expression in epithelial cells. *J Biol Chem*. 2014;289(28):19758–19768. doi:10.1074/jbc.M114.584540
44. Ramnath D, Tunny K, Hohenhaus DM, et al. TLR3 drives IRF6-dependent IL-23p19 expression and p19/EBI3 heterodimer formation in keratinocytes. *Immunol Cell Biol*. 2015;93(9):771–779. doi:10.1038/icb.2015.77
45. Al Hamrashdi M, Brady G. Regulation of IRF3 activation in human antiviral signaling pathways. *Biochem Pharmacol*. 2022;200:115026. doi:10.1016/j.bcp.2022.115026
46. Leach N, Bjerke SL, Christensen DK, et al. Emerin is hyperphosphorylated and redistributed in herpes simplex virus type 1-infected cells in a manner dependent on both UL34 and US3. *J Virol*. 2007;81(19):10792–10803. doi:10.1128/jvi.00196-07
47. Adhikary G, Chew YC, Reece EA, Eckert RL. PKC-delta and -eta, MEKK-1, MEK-6, MEK-3, and p38-delta are essential mediators of the response of normal human epidermal keratinocytes to differentiating agents. *J Invest Dermatol*. 2010;130(8):2017–2030. doi:10.1038/jid.2010.108
48. Chew YC, Adhikary G, Xu W, Wilson GM, Eckert RL. Protein kinase C δ increases Kruppel-like factor 4 protein, which drives involucrin gene transcription in differentiating keratinocytes. *J Biol Chem*. 2013;288(24):17759–17768. doi:10.1074/jbc.M113.477133
49. Liang Y, Liu R, Zhang J, et al. Negative regulation of interferon regulatory factor 6 (IRF6) in interferon and NF-kappaB signalling pathways of common carp (Cyprinus carpio L.). *BMC Vet Res*. 2022;18(1):433. doi:10.1186/s12917-022-03538-4
50. Ahmad I, Wilson DW. HSV-1 cytoplasmic envelopment and egress. *Int J Mol Sci*. 2020;21(17):5969. doi:10.3390/ijms21175969
51. Thery F, Martina L, Asselman C, et al. Ring finger protein 213 assembles into a sensor for ISGylated proteins with antimicrobial activity. *Nat Commun*. 2021;12(1):5772. doi:10.1038/s41467-021-26061-w
52. Pan M, Yin Y, Hu T, et al. UXT attenuates the CGAS-STING1 signaling by targeting STING1 for autophagic degradation. *Autophagy*. 2023;19 (2):440–456. doi:10.1080/15548627.2022.2076192
53. Scholz GM, Sulaiman NS, Al Baiiaty S, Kwa MQ, Reynolds EC. A novel regulatory relationship between RIPK4 and ELF3 in keratinocytes. *Cell Signal*. 2016;28(12):1916–1922. doi:10.1016/j.cellsig.2016.09.006
54. Tanghe G, Urwyler-Rösselet C, De Groote P, et al. RIPK4 activity in keratinocytes is controlled by the SCF(β-TrCP) ubiquitin ligase to maintain cortical actin organization. *Cell Mol Life Sci*. 2018;75(15):2827–2841. doi:10.1007/s00018-018-2763-6